

Preparation and Optimization of Polyaniline /Titanium Dioxide /Carboxymethyl Cellulose Powder for Effective Nickel Adsorption

(Penyediaan dan Pengoptimuman Serbuk Polianilin /Titanium Dioksida /Karboksimetil Selulosa untuk Penjerapan Nikel Berkesan)

MICHELLE LI-YEN LEE¹, ISHAK AHMAD² & SOOK-WAI PHANG^{1,*}

¹*Department of Physical Science, Faculty of Applied Science, Tunku Abdul Rahman University of Management and Technology (TAR UMT), Jalan Genting Klang, Setapak, 53300 Kuala Lumpur, Malaysia*

²*Polymer Research Centre (PORCE), Department of Chemical Sciences, Faculty of Science and Technology, Universiti Kebangsaan Malaysia, 43600 UKM Bangi, Selangor, Malaysia*

Received: 14 March 2024/Accepted: 11 June 2024

ABSTRACT

Hexanoic acid-doped polyaniline (PAni) is a great potential candidate to replace conventional adsorbent towards the removal of heavy metal waste from electroplating industry, especially nickel (Ni). In this study, different weight % (wt %) of titanium dioxide (TiO₂) and carboxymethyl cellulose (CMC) are added to form PAni composites with enhanced Ni removal efficiency. All the synthesized samples were examined with FTIR, UV-Vis, conductivity measurement, XRD, TGA, and FESEM to confirm their chemical structures, oxidation states, electrical conductivity, crystallinity and incorporation of metal oxide, thermal stability, and surface morphology, respectively. Among the different samples, PAni / TiO₂ 20 % exhibited the highest Ni removal efficiency of 37.5 %. Upon further addition of CMC, PAni / TiO₂ / CMC 5 % showed the highest Ni removal efficiency of 89.08 %. Optimization of the experimental parameters were conducted and a maximum Ni removal efficiency of 97.88 % was achieved at pH 10, 30 min contact time at a temperature of 30 °C, and with an adsorbent dosage of 0.01 g. This study shows that the composite of PAni / TiO₂ / CMC 5 % shows good potential to be applied as adsorbent of the removal of Ni ions.

Keywords: Adsorption; carboxymethyl cellulose; nickel; polyaniline; ternary composite

ABSTRAK

Polianilin (PAni) yang didopkan dengan asid heksanoik merupakan calon yang berpotensi besar untuk menggantikan penjerap konvensional ke arah penyingkiran sisa logam berat, terutamanya nikel (Ni), yang berasal daripada sisa industri penyaduran elektrik. Dalam kajian ini, % berat (berat %) titanium dioksida (TiO₂) dan karboksimetil selulosa (CMC) yang berbeza telah digunakan untuk memperoleh komposit PAni yang mempunyai kecekapan penyingkiran Ni yang dipertingkatkan. Semua sampel yang disintesis telah diperiksa dengan FTIR, UV-Vis, ukuran kekonduksian, XRD, TGA dan FESEM untuk mengesahkan struktur kimia mereka, keadaan pengoksidaan, kekonduksian elektrik, kehabluran dan penggabungan oksida logam, kestabilan terma, dan morfologi permukaan masing-masing. Antara sampel yang berbeza, PAni / TiO₂ 20 % menunjukkan kecekapan penyingkiran Ni yang tertinggi iaitu 37.5 %. Selepas penambahan CMC, PAni / TiO₂ / CMC 5 % menunjukkan kecekapan penyingkiran Ni yang tertinggi iaitu 89.08 %. Pengoptimuman parameter uji kaji telah dijalankan dan kecekapan penyingkiran Ni maksimum sebanyak 97.88 % telah dicapai pada pH 10, 30 minit masa sentuhan pada suhu 30 °C dan dengan dos penjerap sebanyak 0.01 g. Kajian ini menunjukkan bahawa komposit PAni / TiO₂ / CMC 5 % menunjukkan potensi yang baik untuk digunakan sebagai penjerap penyingkiran ion Ni.

Kata kunci: Karboksimetil selulosa; komposit ternari; nikel; penjerapan; polianilin

INTRODUCTION

Water is a vital element for all living things and clean waters are critical for the well-being for all organisms. However, in the recent years, the struggle to secure safe

and clean water has been on the rise. As predicted by the World Health Organization (WHO), an alarming figure of more than three billion people will not be able to secure safe water sources by the year of 2025 (Bankole et al.

2019). This is because in this modern era of globalization and industrialization, our environment is constantly exposed to and degraded by pollutants generated by industrial activities such as electroplating, mining, power generation, and metallurgy (Rajoria, Vashishtha & Sangal 2022). Among these, electroplating is one of the trending industries involving the application of a metal layer onto the surface of another material with the goal of extending the material's shelf life against corrosion (Rahman et al. 2021). Nickel (Ni) is one of the heavy metals that is widely used as a protective coating on materials such as stainless steel or metal alloys and as decorative finish due to its glossy finishing (Costa, Costa & Neto 2022).

In fact, among all heavy metals, Ni is one of the most heavily produced base metals accounting to a total amount of 2.7 million tonnes in year 2019, presenting great disposal challenges due to its high persistency and toxicity towards living cells, crops, and aquatic lives (Noman et al. 2022). Chang et al. (2006) reported Ni (II) concentration of 1.74 to 22.73 $\mu\text{g/L}$ in the urine of electroplating industry workers, and this could potentially lead to health issues such brain, spinal cord, and human internal organs damages (Chang et al. 2006; Li et al. 2023). Conventional treatment methods such as coagulation, membrane filtration, and ion exchange often require long processing hours and high operation, inflicting high costs and low efficiency (Noman et al. 2022). The adsorption method, on the other hand, attracts greater attention due to its environmentally friendly operation, flexibility on choice of adsorbent, high efficiency, and regeneration ability of adsorbent (Kruszelnicka et al. 2022).

Different types of adsorbents are commonly employed, ranging from mineral adsorbents, carbon-based adsorbents, to biosorbents with examples such as activated carbon, zeolites, and graphene (Qasem, Mohammed & Lawal 2021). However, these conventional adsorbents require high costs for their materials and involve cumbersome processes. For instance, activated carbon, despite its high efficiency, is cost-ineffective in terms of recyclability (Moosavi et al. 2020). Therefore, alternative adsorbents that are more economical and practical for large scale usage are worth venturing into. Conducting polymer (CP) based adsorbents have drawn the attention of researchers due to their good adsorption potential, easily synthesized, and their conjugated π -bond systems render them unique electrical, optical, and physical properties (Khan et al. 2021).

Among different CPs, polyaniline (PAni) shows great potential to be applied as contaminant adsorbent owing

to its low monomer cost, easy synthesis, modifiable properties and backbone for regeneration, and porous structure for efficiency (Ajeel & Kareem 2019). For instance, the work of Samadi et al. (2021) saw a removal efficiency of 263.3 mg/g of Cr^{6+} by PAni nanosheets. As PAni exhibits some disadvantages when used on its own as adsorbent, such as poor mechanical strength and limited efficiency, the composites of PAni with other materials are also widely studied. To illustrate, Debnath et al. (2015) discovered that when PAni was coupled with lignocellulose, the adsorption of Congo red dye achieved was 1672.5 mg/g (Debnath et al. 2015; Zare, Motahari & Sillanpaa 2018). In addition, when coupled with kapok fibre and graphene oxide, the PAni composites were able to adsorb 66.2 mg/g of Cr^{6+} and 210 mg/g of Zn^{2+} , respectively (Samadi et al. 2021).

In this study, titanium dioxide (TiO_2) and carboxymethyl cellulose (CMC) are chosen to form composite with PAni to achieve the maximum removal efficiency of Ni. With the addition of TiO_2 , the charge transport and surface roughness of the composite is aimed to be improved, thus enhancing the electrostatic attraction and maximizing the surface area for adsorption of Ni^{2+} . In addition, with the incorporation of CMC, which is a biodegradable polymer with good mechanical property, the mechanical property and sustainability value of the PAni composite can be improved, while obtaining additional active sites from CMC for the adsorption of Ni^{2+} . As of the best knowledge of the author, the application of the ternary system of PAni / TiO_2 / CMC for the removal of Ni and other heavy metals produced from electroplating is a new area to be explored. The closest work done is the use of PAni / TiO_2 / CMC towards dye adsorption by Tanzifi et al. (2018) while this study focuses on Ni and other heavy metals used in electroplating while optimizing the experimental parameters to achieve the best possible removal efficiency.

MATERIALS AND METHODS

MATERIALS

Aniline (Ani) with purity $\geq 99.9\%$ and ammonium persulphate (APS) with purity $\geq 98.0\%$ from Sigma Aldrich were used as monomer and oxidant, respectively. In addition, hexanoic acid (HA) dopant with purity $\geq 98.0\%$ and titanium dioxide (TiO_2) nanoparticle (P25) (particle size $< 30\text{ nm}$) were also purchased from Sigma Aldrich. On the other hand, microcrystalline cellulose was purchased from Chem Soln. Isopropanol (IPA) with purity $\geq 99.8\%$ was obtained from Chemiz to dissolve the

microcrystalline cellulose. Then, to obtain carboxymethyl cellulose (CMC) from microcrystalline cellulose, sodium hydroxide (NaOH) with purity $\geq 99.0\%$ purchased from Merck Germany and sodium chloroacetate with purity $\geq 98.0\%$ from Sigma Aldrich were used. Besides, ethanol (EtOH) with a purity of $\geq 99.5\%$ from System was used to terminate the reaction. For the washing of all synthesized PANi samples, methanol (MeOH) with purity $\geq 99.9\%$ from Chemiz was used. In addition, all usage of distilled water in this research study was obtained from the laboratory distillation system. For the preparation of heavy metal stock solution, nickel (II) chloride hexahydrate ($\text{NiCl}_2 \cdot 6\text{H}_2\text{O}$) with a purity of $\geq 98.0\%$ was obtained from Chem Soln.

SYNTHESIS METHODS

Hexanoic acid-doped polyaniline (PANi) was synthesized by first adding 1250 μL of HA into distilled water and stirred to ensure homogeneity. Then, 915 μL of Ani monomer was added dropwise into the solution. The solution was maintained at 0°C in an ice box where the temperature was measured at fixed intervals and kept under continuous stirring to ensure homogeneity of the solution. Then, 2.28 g of APS was dissolved using cold distilled water. The APS solution was slowly dropped into the monomer solution to initiate the polymerization. Following the completion of the addition of APS solution, the mixture was stirred for another hour to ensure a homogeneous dispersion. After that, the stirring was stopped and the polymerization was allowed to take place overnight. Following that, to obtain the synthesized solid PANi, the mixture was washed with distilled water and MeOH and the PANi obtained was dried in the oven overnight.

To synthesize PANi / TiO_2 composite, similar amount of HA and Ani were added and prepared as described above. After that, 5 weight % (wt %) of TiO_2 was slowly added into the solution and the mixture was kept under continuous stirring for overnight. Then, APS solution was similarly added to initiate the polymerization process as described above for PANi. Lastly, the washing and drying of the synthesized PANi / TiO_2 followed the similar procedure as described above. The entire procedure was repeated by replacing 5 wt % of TiO_2 with 10, 20, and 30 wt % of TiO_2 to synthesize PANi / TiO_2 with different wt %.

Microcrystalline cellulose was used to prepared CMC through the process of carboxymethylation. Firstly, 5 g of microcrystalline cellulose was added into IPA and the solution was stirred for homogeneity. Next, 20 %

NaOH solution was added and the solution was stirred for 1.5 h. Then, 3 g of sodium chloroacetate was added in and the mixture was further stirred. After that, the beaker containing the mixture was kept in an oven for 2.5 h. The solid obtained was suspended in EtOH while the liquid was discarded. Then, the CMC precipitate obtained was filtered and washed with MeOH thrice. Lastly, the CMC precipitate was allowed to dry overnight in an oven.

For the synthesis of PANi / TiO_2 / CMC, similar amount of HA and Ani were added and prepared as discussed. The mixture was continuously stirred and kept at 0°C to ensure homogeneity. Next, the optimized wt % of TiO_2 (in this case, 20 wt %) was slowly added into the mixture under constant stirring. Following that, 5 wt % of the obtained CMC was slowly added into the mixture under continuous stirring. This mixture was then left for overnight stirring. On the next day, APS solution was slowly added into the mixture to initiate the polymerization process as described for PANi. Then, the synthesized PANi / TiO_2 / CMC underwent the similar washing and drying processes as mentioned earlier.

CHARACTERIZATION TECHNIQUES

Fourier Transform Infrared Spectrometry (FTIR) was used to investigate the chemical structures and functional groups of all the synthesized samples. The samples were scanned within the wavenumber range of $650 - 4000\text{ cm}^{-1}$ using Perkin Elmer Spectrum 100 FTIR-ATR. Besides, the oxidation states of the synthesized samples were examined through Ultraviolet-Visible (UV-Vis) spectrophotometry of which the samples were measured within the wavelength range of $250 - 900\text{ nm}$ using Hitachi UH5300 spectrophotometer. On the other hand, Mitsubishi Loresta GX MCP-T700 was used to measure the electrical conductivity of all synthesized samples through the use of a four-point PSP probe. In addition, Field Emission Scanning Electron Microscopy (FESEM) was utilized to examine the morphologies of the samples under the magnification of $10,000 \times$ to $50,000 \times$ through ZEISS Gemini Auriga.

After the addition of TiO_2 into the PANi composites, the elemental compositions of the samples were determined using Energy Dispersive X-ray analysis (EDX) through EDAX to ensure the successful incorporation of TiO_2 into the composite. Also, Thermogravimetry Analysis (TGA) was used to examine the thermal stabilities of the samples by ramping the temperatures from 30°C to 750°C under a heating rate of $20^\circ\text{C}/\text{min}$ using TGA-TA Q50 in a nitrogen environment. In addition, to examine the

crystallographic information of the samples, especially after the incorporation of TiO₂ and carboxymethylation of cellulose, X-ray Diffraction (XRD) analysis with 2θ from 5° to 80° was utilized through Bruker D8 Advance. Lastly, the concentrations of Ni in solutions were measured using Flame Atomic Absorption Spectroscopy (FAAS) by Thermo Scientific iCE 3000 series.

HEAVY METAL REMOVAL

A calibration curve was first built using Ni solutions. Then, fixed amount of the different PANi sample (PANi, PANi / TiO₂, or PANi / TiO₂ / CMC) was added into 12 ppm Ni solution. The adsorption of Ni onto the PANi sample was allowed to take place under continuous shaking at room temperature. Then, the mixture was centrifuged, filtered, and the filtrate was measured for its Ni concentration using FAAS. The heavy metal removal efficiencies of the different PANi samples were determined using Equation (1):

$$\text{Heavy metal removal efficiency (\%)} = \frac{C_i - C_f}{C_i} \times 100 \quad (1)$$

where C_i is the initial Ni concentration before adsorption; and C_f is the final Ni concentration after adsorption. In order to achieve maximum Ni removal efficiency, the different experimental parameters of pH, contact time, temperature, and adsorbent weight were studied and optimized.

RESULTS AND DISCUSSION

FTIR ANALYSIS

Figure 1 shows the FTIR spectra obtained for microcrystalline cellulose, synthesized CMC, PANi, PANi incorporated with different wt % of TiO₂, and PANi / TiO₂ added with 5 wt % of CMC when measured from 650 – 4000 cm⁻¹. Firstly, the peak observed at 782 cm⁻¹ is contributed by the bending vibration of out-of-plane aromatic C-H group formed during the protonation of PANi (Yadav, Mohammad & Khanna 2023). Besides, the broad peak observed at 1030 cm⁻¹ is due to the in-plane bending of the PANi aromatic C-H groups (Jayamurugan et al. 2020). In addition, the peak at 1292 cm⁻¹ represents the C-N stretching of secondary aromatic amine or benzenoid ring of PANi (Helmy et al. 2021; Jayamurugan et al. 2020). The peaks at 1460 cm⁻¹ and 1554 cm⁻¹ represent the significant C=C stretching vibration of benzenoid and quinoid rings of PANi, respectively (L

et al. 2023). Lastly, the peaks at 2905 cm⁻¹ and 3210 cm⁻¹ are attributed to the stretching vibration of C-H and stretching vibration of N-H groups in PANi, respectively (Anju & Narayanankutty 2018; Budi et al. 2017). All in all, the FTIR spectrum of PANi has confirmed the chemical structure of PANi.

Upon addition of TiO₂ into the PANi system, it was found that the overall peaks of PANi / TiO₂ have shifted to a slightly higher wavenumber. For instance, the peak caused by the bending vibration of out-of-plane aromatic C-H group has shifted from 782 cm⁻¹ to 787 – 792 cm⁻¹ while that of in-plane bending of aromatic C-H group has shifted from 1030 cm⁻¹ to 1035 – 1069 cm⁻¹. In addition, the C-N stretching peak of secondary aromatic amine has shifted from 1292 cm⁻¹ to 1292 – 1297 cm⁻¹ while that of C=C stretching vibration of benzenoid and quinoid rings have shifted from 1460 cm⁻¹ and 1554 cm⁻¹ to 1475 – 1485 cm⁻¹ and 1559 – 1564 cm⁻¹, respectively. Finally, the peaks of C-H stretching and N-H stretching have shift from 2905 cm⁻¹ and 3210 cm⁻¹ to 2915 – 2920 cm⁻¹ and 3212 – 3232 cm⁻¹, respectively. The reason for this shift can be attributed to the Coulomb force which has resulted from the interaction between PANi and the TiO₂ particles, as similarly observed by Abid and Hasan (2022), thus, supported the successful incorporation of TiO₂ into the system.

On the other hand, a broader hydroxy -OH peak is exhibited at a slightly higher wavenumber of 3453 cm⁻¹ for CMC compared to at 3330 cm⁻¹ for cellulose. This could be due to the presence of stronger hydrogen bonds in CMC with the addition of carboxylic acid groups (Yuwono et al. 2020). Besides, two significantly different peaks are observed in CMC at 1428 cm⁻¹ and 1576 cm⁻¹ due to the addition of methylene -CH₂ and carbonyl C=O groups, respectively, compared to that of cellulose (Yuwono et al. 2020). Therefore, there was a successful carboxymethylation of microcrystalline cellulose to CMC. As shown in Figure 1, the characteristic peaks of PANi are still observed after the addition of CMC, indicating that the chemical structure of PANi remains unaffected by the incorporation of CMC. However, the peak at 3227 – 3242 cm⁻¹ has become more intense for PANi / TiO₂ / CMC compared to PANi and PANi / TiO₂ due to the hydrogen bond interactions between the -NH groups of PANi and the -OH groups of CMC, which confirms the successful incorporation of CMC into the system (Li et al. 2017). In addition, the stronger peak observed at 1723 – 1728 cm⁻¹ in PANi / TiO₂ / CMC is contributed by the -COOH carboxylic acid groups of CMC (Li et al. 2017). Besides,

there is an overlap of peaks between the stretching vibration of benzenoid and quinoid rings of PANi with that of the methylene and carbonyl groups of CMC at the range of $1400 - 1600 \text{ cm}^{-1}$. All in all, the FTIR spectra obtained have showed interaction between PANi or PANi / TiO_2 with CMC and ascertained the composite formation of PANi / TiO_2 / CMC.

UV-VIS ANALYSIS

UV-Vis spectroscopy is used to examine the level of oxidation and protonation of the synthesized PANi samples. Figure 2 exhibits the UV-Vis spectra of PANi, PANi with different wt % of TiO_2 , and PANi / TiO_2 with 5 wt % of CMC from 250 nm to 900 nm. As shown by the spectrum of PANi, three significant absorptions are observed. The absorption peak at 367 nm is caused by the $\pi - \pi^*$ transition of the benzenoid ring in PANi backbone while the absorption peak at 447 nm is contributed by the polaron - π^* transition (Lv et al. 2023). On top of that, a tailing peak is observed to start around 700 nm which could be contributed by the $\pi - \text{polaron}$ transition of PANi quinoid ring (Lv et al. 2023). These absorption

peaks show that PANi has been successfully synthesized in the conducting emeraldine salt state.

On the other hand, TiO_2 and CMC mainly absorb in the UV wavelength range while its absorption in the visible wavelength range is negligible (Aboelkheir et al. 2022; Monfared & Jamshidi 2019). However, as shown by the spectra of PANi with different wt % of TiO_2 , the composite is observed to be able to absorb in both UV and visible wavelength range. Due to the presence of PANi in the composite, the overall absorption of the composite is shifted to higher wavelengths, causing a redshift from 367 nm to 372 - 382 nm and 447 nm to 460 - 462 nm when compared to pristine PANi (Monfared & Jamshidi 2019). This indicates the successful incorporation and interaction between PANi and TiO_2 . In comparison, upon addition of CMC, there is a significant blueshift of the absorption peaks to a lower wavelength. The peak at 322 - 334 nm is attributed to the combination of PANi and CMC (Aboelkheir et al. 2022). With an increase in the wt % of CMC, the maximum absorption has slightly shifted to a longer wavelength, indicating a decrease in binding energy and thus a better charge delocalization (Aboelkheir et al. 2022).

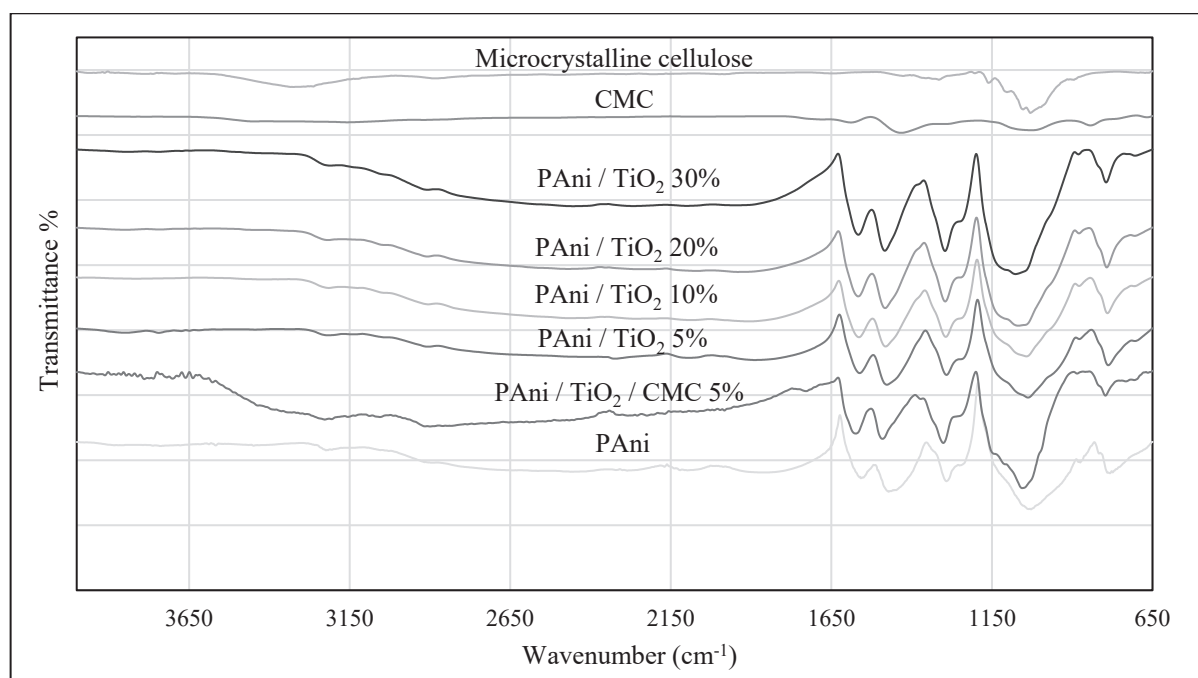


FIGURE 1. FTIR spectra of microcrystalline cellulose, synthesized CMC, PANi, PANi with different wt % of TiO_2 , and PANi / TiO_2 with 5 wt % of CMC

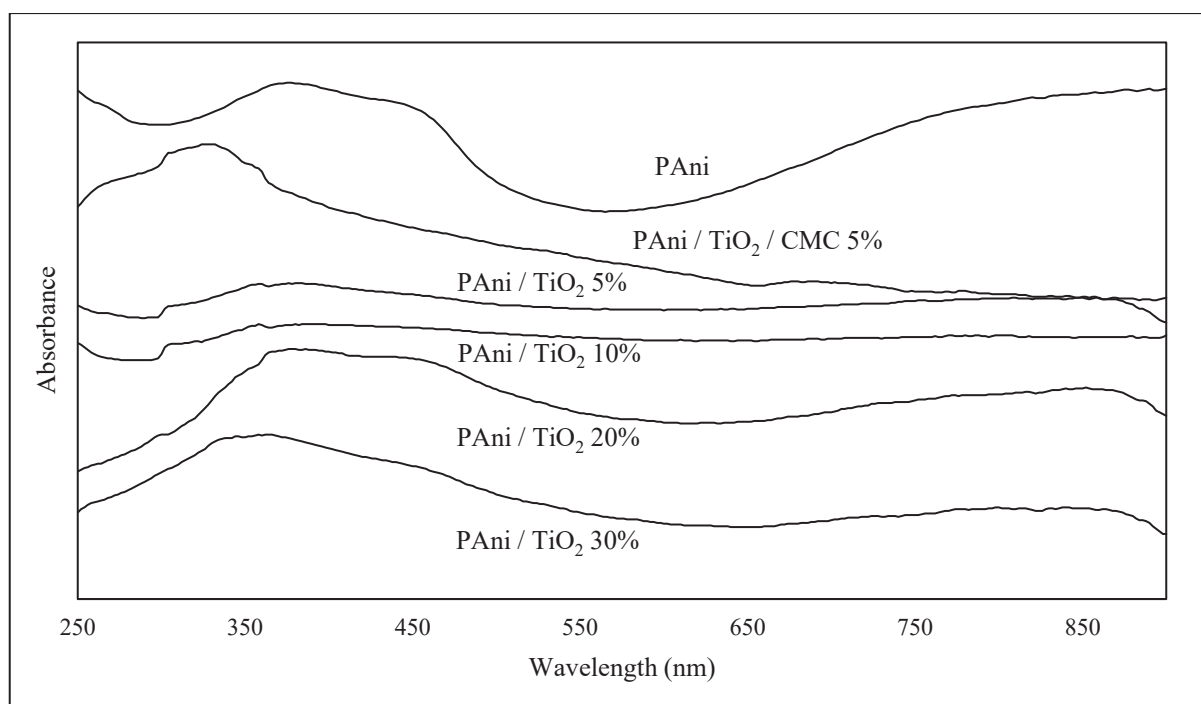


FIGURE 2. UV-Vis spectra of PANi, PANi with different wt % of TiO_2 , and PANi / TiO_2 with 5 wt % of CMC

ELECTRICAL CONDUCTIVITY MEASUREMENT

Figure 3 shows the electrical conductivity measured using the four-point probe method for PANi, PANi with different wt % of TiO_2 , and PANi / TiO_2 with 5 wt % of CMC. It is exhibited that upon addition of TiO_2 , the electrical conductivity of PANi is enhanced from 0.0344 S/cm to 0.0650 S/cm at 20 wt % TiO_2 , followed by a decrease to 0.0179 S/cm when the wt % of TiO_2 reaches 30%. With the p-type nature of PANi and n-type nature of TiO_2 , an interfacial p-n heterojunction is formed (Megha et al. 2018). Due to this, there may have been less bond formation between the N-H group of PANi with the -O group of TiO_2 and thus the PANi chains are allowed to grow longer. Therefore, there is a greater mobility for the charge carriers to hop along the PANi backbone and thus increasing the electrical conductivity of the composite (Megha et al. 2018). When the wt % of TiO_2 reached 30%, the decrease in electrical conductivity can be explained by the fact that with increased amount of TiO_2 , there is more bond formation between PANi and TiO_2 , thus hindered the conjugation lengths in the PANi chains (Su et al. 2007). Besides, the charge transport along PANi chain may have also been hindered by the increase TiO_2 particles (Su et al. 2007).

On the other hand, the electrical conductivity was found to have decreased to only 0.0157 S/cm after the addition of CMC into the PANi / TiO_2 system. This could be due to the reason that upon addition of amorphous CMC, the crystallinity of PANi / TiO_2 system is decreased and hence hindered the charge carrier mobility (Scholes et al. 2017). This can also be seen from Figure 2 where a blueshift is observed for PANi / TiO_2 / CMC compared to PANi and this could be due to the proximity between the anions and polarons of the system which causes a more localized polarons and hence lower electrical conductivity (Scholes et al. 2017). With this decrease in crystallinity of the composite system, there is an increase in surface area and thus increase in the number of active sites on the surface of the composite system, which leads to an enhanced Ni removal efficiency as observed in this study (Wei et al. 2015).

XRD ANALYSIS

XRD was used to study and compare the crystallinity of PANi, PANi / TiO_2 20 %, PANi / TiO_2 / CMC 20 %, microcrystalline cellulose, CMC, and nano TiO_2 at 2θ of 5° to 80° as shown in Figure 4. PANi exhibited three peaks at $2\theta = 15.56^\circ$ and 20.84° , which are contributed

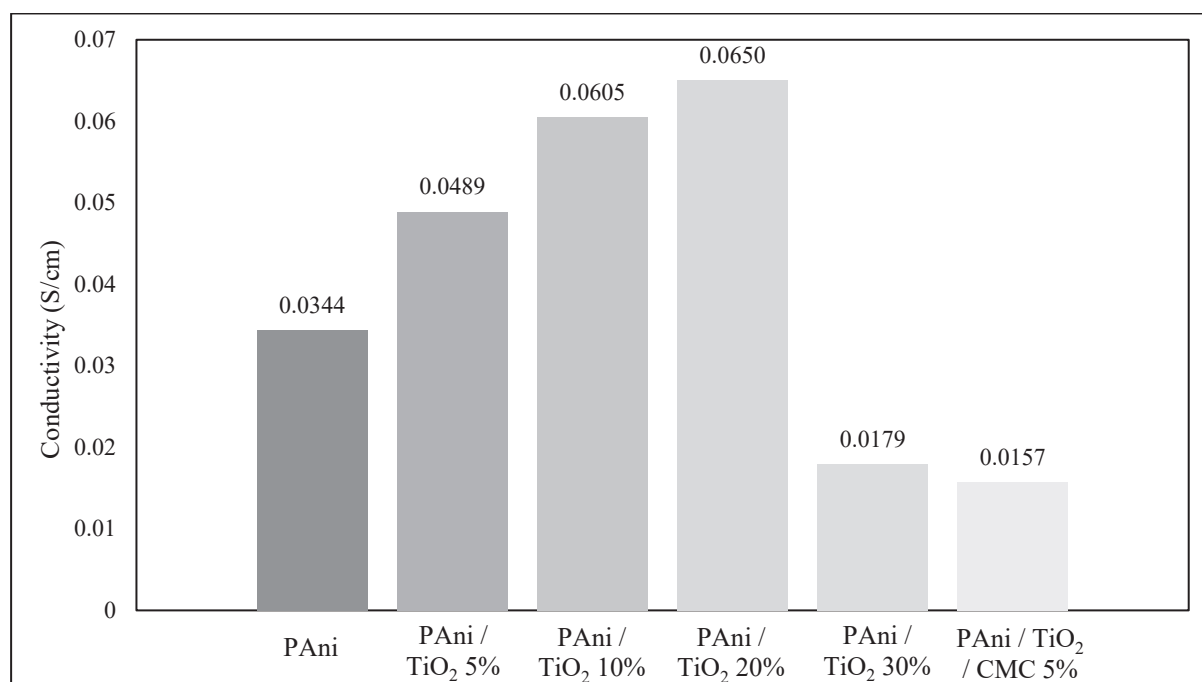


FIGURE 3. Electrical conductivity measurement of PANi, PANi with different wt % of TiO₂, and PANi / TiO₂ with 5 wt % of CMC

by the periodicity parallel to the PANi chains, and 25.35° which is due to the periodicity perpendicular to PANi chains (Megha et al. 2017). On the other hand, the diffractogram of nano TiO₂ shows the characteristic peaks of TiO₂ anatase with 2θ of 25.25°, 37.73°, 48.14°, and 53.79° corresponding to the 101, 103, 200, and 105 planes, respectively (Monfared & Jamshidi 2019). As shown in Figure 4, two amorphous peaks at 2θ of 15.44° and 22.71° are observed for microcrystalline cellulose whereas only one amorphous peak at 2θ of 20.07° is observed for CMC. This shows the successful carboxymethylation of microcrystalline cellulose to CMC with the crystallinity of microcrystalline cellulose being decreased due to the breakage of hydrogen bonds and the addition of carboxymethyl groups in CMC (Costa et al. 2022). The diffractogram of PANi / TiO₂ 20% and PANi / TiO₂ / CMC 20% showed that the peaks of PANi and CMC have been completely overshadowed by the strong characteristic peaks of TiO₂ with no shifts or additional peaks observed. This shows the successful incorporation of TiO₂ into the composite system. Following the TiO₂ incorporation, the electrical conductivity and surface roughness of the system were enhanced, and an increased Ni removal efficiency was observed due to the enhanced

crystallinity contributed by TiO₂. However, when a wt % of 30 wt % TiO₂ was reached, the charge transport and active sites along the polymer chain may have been hindered by the increased TiO₂ deposits which eventually caused a decrease in the Ni removal efficiency.

TGA ANALYSIS

TGA was conducted to examine the thermal stability of the samples when subjected to high temperature in a controlled environment. A comparison of the results obtained for pristine PANi, nano TiO₂, and upon addition of fixed wt % of TiO₂ and CMC is shown in Figure 5 to discuss the effects TiO₂ and CMC have towards the thermal stability of the PANi composite. As expected, pristine TiO₂ exhibited high thermal stability of mineral with a negligible weight loss of less than 2%, which could be attributed to the loss of adsorbed water or moisture (Monfared & Jamshidi 2019). On the other hand, PANi showed three main decomposition steps and the first step which occurred below 160 °C could be caused by the loss of adsorbed water or trace methanol from the polymer structure (Monfared & Jamshidi 2019). The second decomposition step which happened

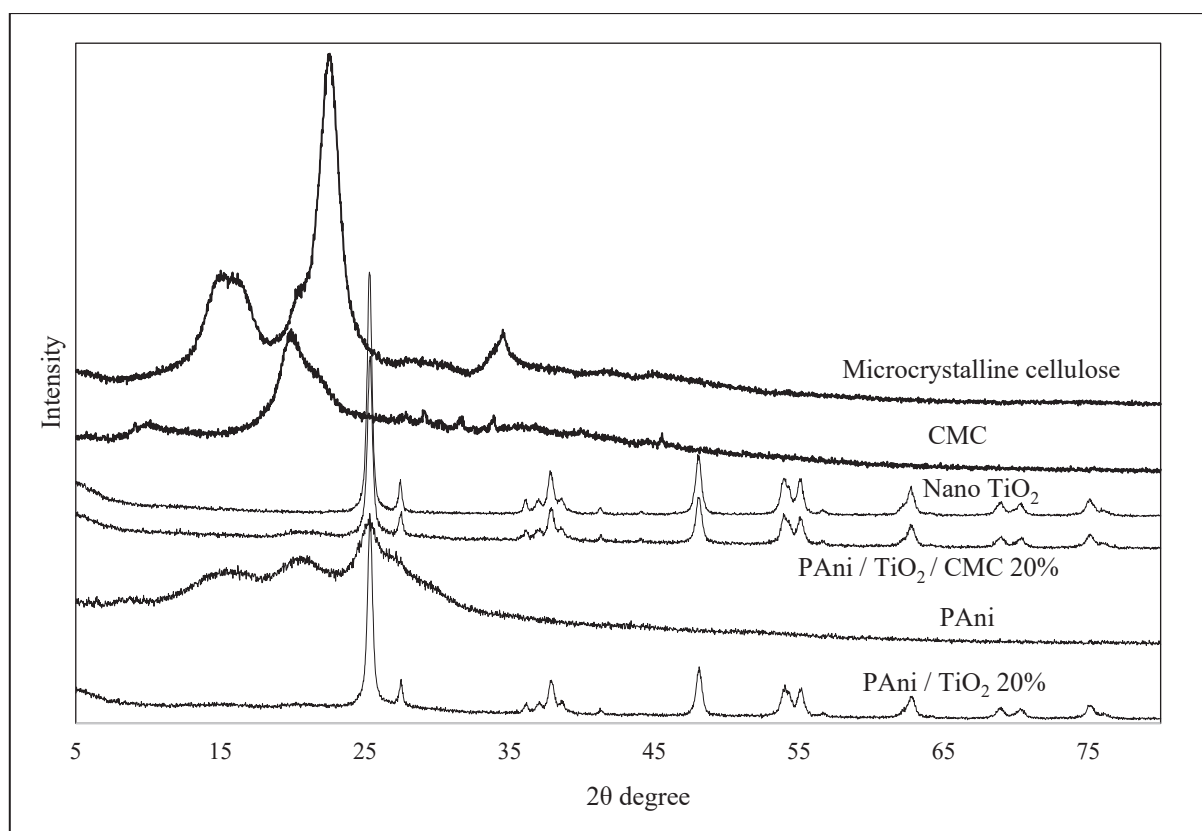


FIGURE 4. XRD diffractogram of PANi, PANi / TiO₂ 20%, PANi / TiO₂ / CMC 20 %, microcrystalline cellulose, CMC, and nano TiO₂

rapidly from around 160 – 500 °C is caused by the loss of dopant, breaking of functional groups and bonds that formed the PANi chain (Sambaza, Maity & Pillay 2020). Finally, the last decomposition is due to the degradation of the polymer backbone or of the carbonaceous material (Monfared & Jamshidi 2019).

As shown by Figure 5, the addition of TiO₂ has significantly improved the thermal stability of PANi. This can be seen from the change in weight % from 68.95 % of PANi to 82.02 % of PANi / TiO₂ 20 % for decomposition before 500 °C. Subsequently, the residual % had also increased from 54.67 % of PANi to 73.29 % of PANi / TiO₂ 20 %. This shows the successful incorporation of TiO₂ and the interaction between PANi and TiO₂ to improve the composite's thermal stability. Upon addition of CMC, the first decomposition step of below 160 °C showed no major changes. However, at temperature beyond 300 °C, the loss of -COO groups of CMC had caused a rapid weight loss in PANi / TiO₂ / CMC 5% (Olad et al. 2021). Nevertheless, the final residual % of the composite system

is still higher compared to that of pristine PANi, with 76.72 % for PANi / TiO₂ / CMC 5 % compared to 56.11 % for PANi, indicating the enhanced thermal strength of the composite due to the inclusion of TiO₂ and CMC chains.

FESEM ANALYSIS

The morphologies of the synthesized samples were examined using FESEM at 50,000x magnification and are shown in Figure 6. PANi with a longitudinal and tubular-like structure (as shown by the red circle in Figure 6(a) was formed at low temperature of 0 °C under static polymerization condition. Alongside with the slow addition of APS oxidant, the polymerization rate was suppressed to allow the polymer to grow slowly in an orderly manner with minimum defects (Tale, Nemade & Tekade 2021). In addition, Figure 10(b) and 10(c) shows clear deposition of white TiO₂ particles on the polymer structure. It can be seen that when observed at the same magnification of 50,000x, as the wt % of TiO₂ increased, the size of the polymer structure has decreased. This

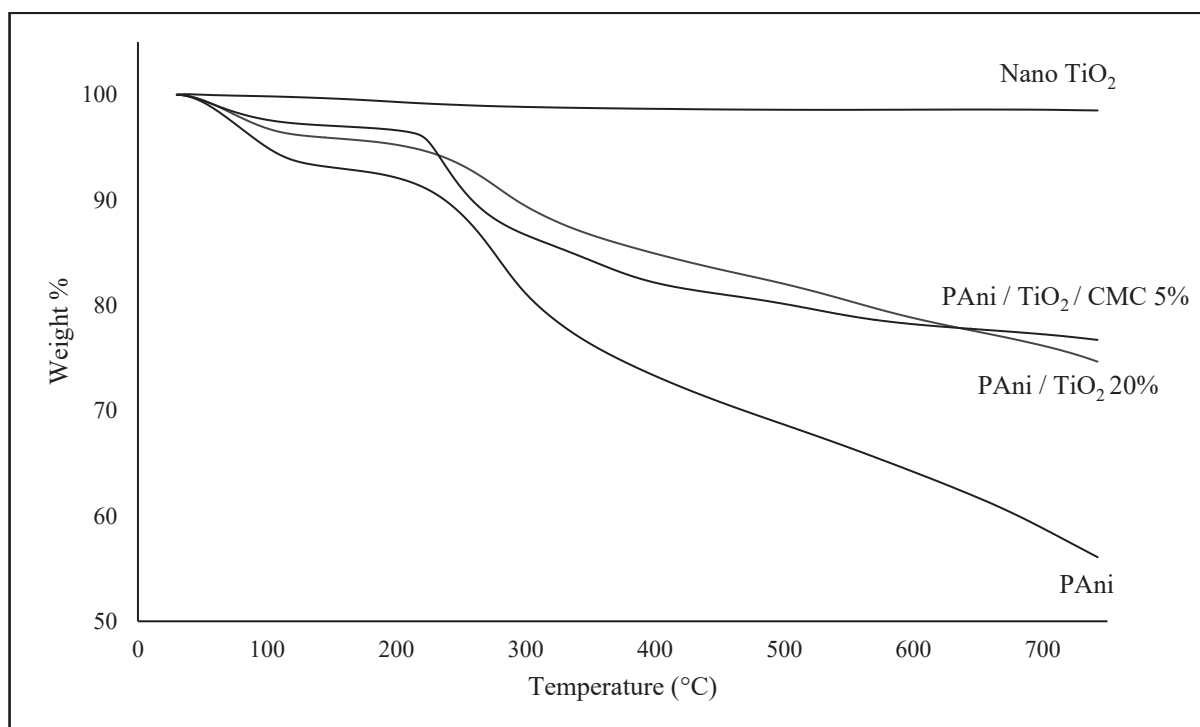


FIGURE 5. Thermogram of PAni, nano TiO₂, PAni / TiO₂ 20 %, and PAni / TiO₂ / CMC 5 %

could be due to the strong hydrogen bonds that form between the -O groups of TiO₂ and -NH groups of PAni, which also explains the growing agglomeration of TiO₂ on the PAni structure (Andreas, Irmanto & Oktaviani 2022). Besides, with the further addition of CMC, more globular appearance is observed and the polymer structure appears to be more compact and rougher. This observation agrees with the work of Barik et al. (2010) where it was concluded that this is caused by the binding of CMC on PAni structure through electrostatic interactions. Overall, the smaller particle size caused by addition of TiO₂ and the rougher surface caused by TiO₂ and CMC contribute to a bigger surface area, allowing more binding sites to adsorb Ni ions.

Ni REMOVAL EFFICIENCY

Figure 7 shows the Ni removal efficiency of PAni, PAni with different wt % of TiO₂, and PAni with 5 wt % of CMC. With increasing wt % of TiO₂, the Ni removal efficiency was improved from 31.25 % of pristine PAni to 37.50 % of PAni / TiO₂ 20 %. This can be attributed to the smaller particle structure and rougher surface of PAni / TiO₂ composite which allowed a bigger surface area and more active sites for the binding of Ni ions (Barik et

al. 2010). As the wt % of TiO₂ reached 30 %, there was a drop in the Ni removal efficiency, and this could be due to the reason that the increased amount of TiO₂ had caused the TiO₂ to agglomerate on top of the polymer structure, as seen in Figure 6(c), rather than being dispersed and deposited evenly on the polymer structure. This may have blocked the effective interaction and adsorption of Ni ions by the composite structure. In addition, the increased crystallinity upon further addition of TiO₂ may have caused the pore structure to be so rigid that it limits the sorption of Ni into the composite structure (Deesaen 2015). Therefore, the wt % of 20 % TiO₂ was chosen to subsequently form PAni / TiO₂ / CMC composite.

Furthermore, highest Ni removal efficiency was achieved by PAni / TiO₂ / CMC 5 % at 89.08 %. As CMC is very hydrophilic in nature, it hydrolyses completely in the acidic Ani solution during synthesis and the neutral -COONa groups are dissociated into the negatively charged -COO groups (Peng et al. 2012). Thereafter, the -COO groups of CMC easily bond with the -NH groups of PAni through electrostatic interaction (Peng et al. 2012). Due to the hydrophilicity of CMC and the favoured interaction between the -COO groups of CMC and -NH groups of PAni, more globular appearance and compact

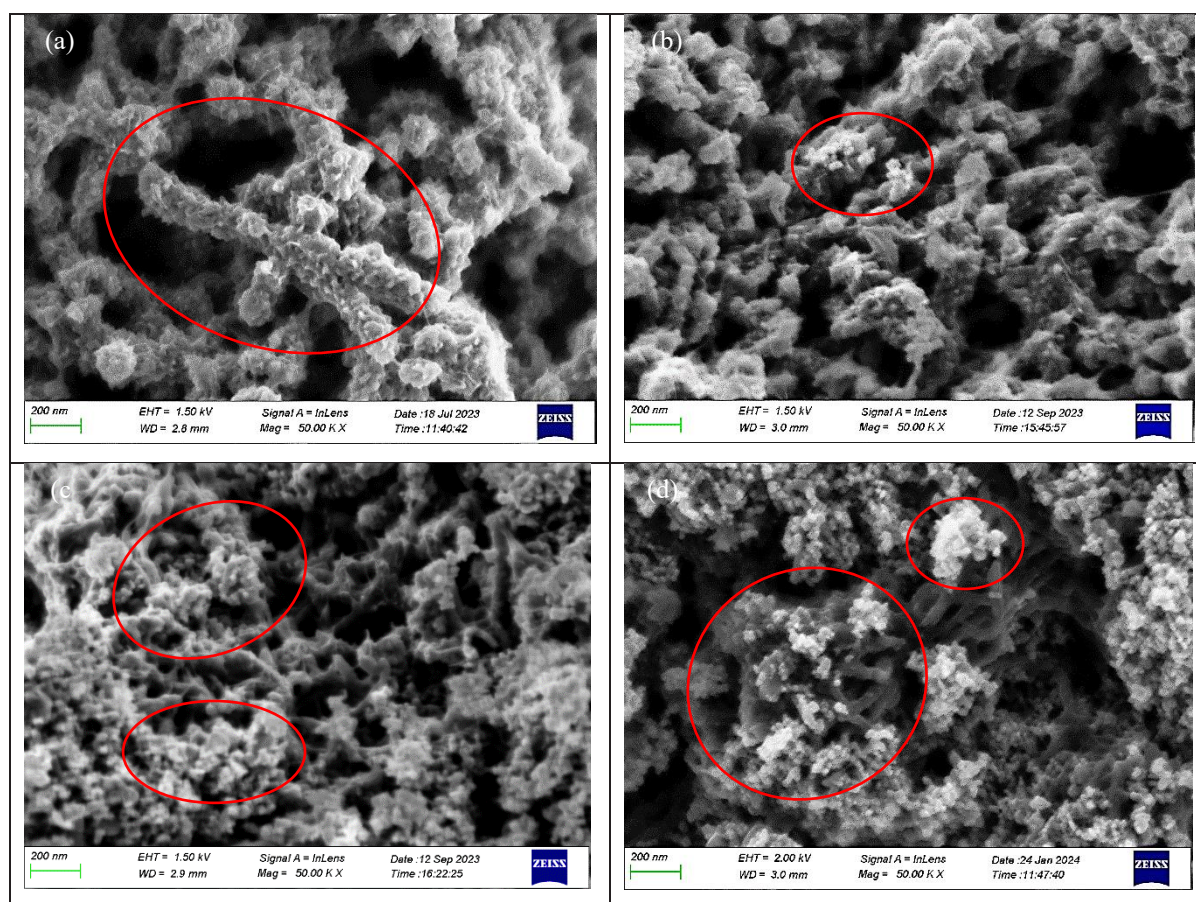


FIGURE 6. FESEM images of (a) PANi (b) PANi / TiO₂ 5 % (c) PANi / TiO₂ 30 % (d) PANi / TiO₂ / CMC 5 % at 50,000 magnification

polymer structure can be seen in Figure 6(d) following further addition of CMC (Barik et al. 2010). Therefore, further addition of CMC of more than 5 wt % favoured the interaction between CMC and PANi instead of the interaction between the active sites of CMC or PANi with that of Ni (II) ions. Nonetheless, the Ni removal efficiency was improved from 37.50 % of PANi / TiO₂ 20% to 89.08 % of PANi / TiO₂ / CMC 5 % as the long chain structure of CMC containing various -OH and -COO groups which act as additional active sites for the adsorption of Ni²⁺ (Singh et al. 2023). Besides, as the emeraldine PANi backbone contains both positively-charged and electron rich sites of nitrogen atoms, the positively-charged sites, which originally repels Ni²⁺, can now be fully utilized to form interaction with TiO₂ and CMC to adsorb Ni²⁺, thus maximizing the PANi backbone for adsorption. Figure 8 shows the proposed molecular structure of the PANi composite and the adsorption of Ni²⁺ ion onto the composite structure.

OPTIMIZATION OF EXPERIMENTAL PARAMETERS FOR NI REMOVAL

Figure 9 shows the Ni removal efficiency of PANi / TiO₂ / CMC 5 % at different pH of 5, 7, and 10 which represents the acidic, neutral, and basic conditions respectively. For heavy metal adsorption, pH plays a vital role as it affects the adsorbent surface charge which subsequently influence the interaction between the adsorbent surface and the heavy metal ion (Arsalan et al. 2022). At low pH, the Ni removal efficiency of the PANi composite was limited at 10.49 % - 10.87 % as there is a competition between the H⁺ ions in the solution and the Ni²⁺ ions with the active sites of the composite, thus reducing the successful adsorption of Ni. At basic pH, the Ni removal efficiency was able to achieve 31.25 % without the occurrence of metal precipitation. This shows that a basic pH is preferred for the adsorption of Ni by the PANi composite as there is no competing species and

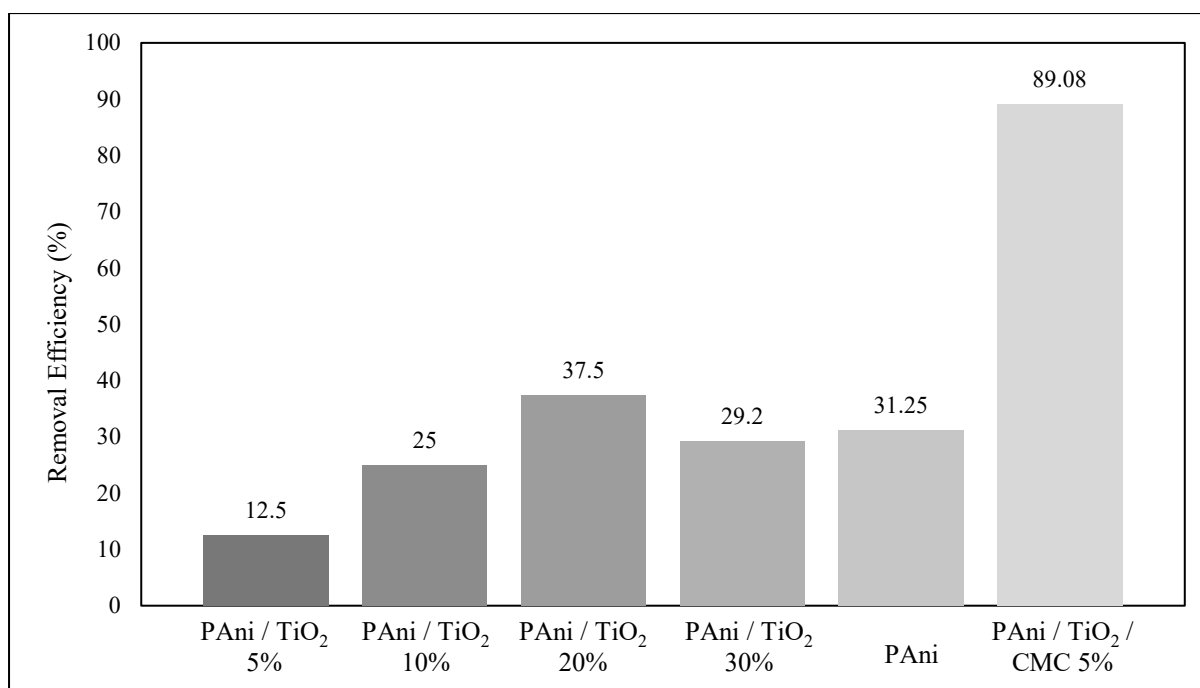


FIGURE 7. Ni removal efficiency of PANi, PANi with different wt % of TiO₂, and PANi with 5 wt % of CMC

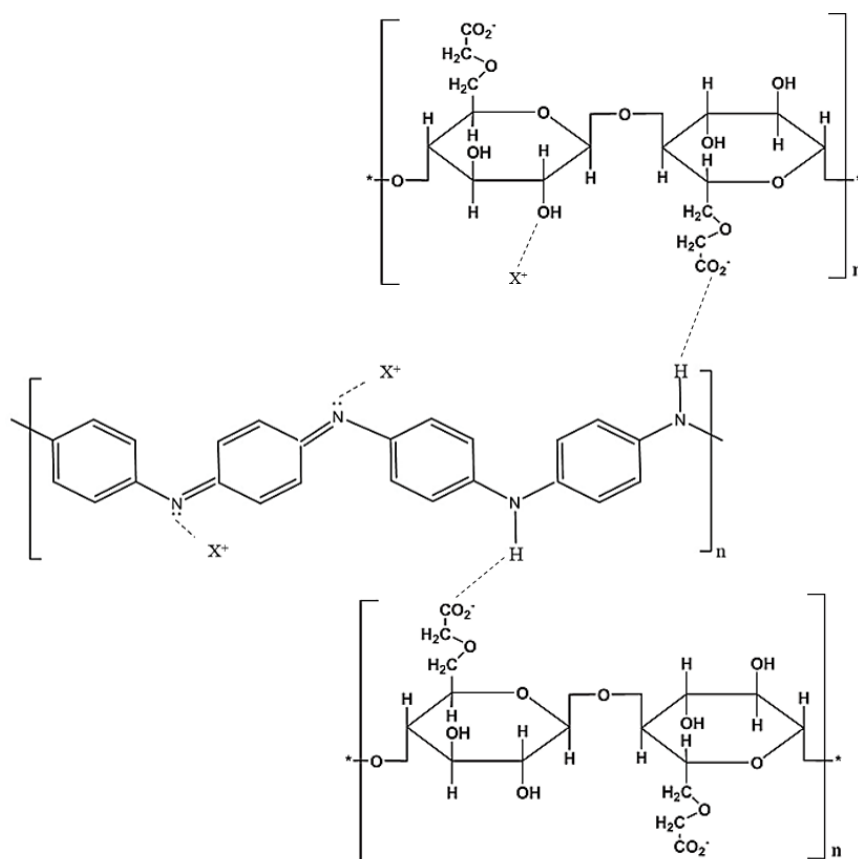


FIGURE 8. Proposed molecular structure of PANi composite and adsorption of Ni (represented by X⁺)

thus a better adsorption can be achieved. Subsequent experiments were conducted at pH 10 to examine the effects of other experimental parameters towards the removal efficiency of Ni.

Figure 10 shows the Ni removal efficiency of PANi / TiO₂ / CMC 5 % against different contact time of 5, 10, 30, 60, 180, and 360 min. A maximum Ni removal efficiency of 86.59 % was achieved at 30 min, after which the removal efficiency saw a slight dip and ultimately reaches an equilibrium. This shows that approximately 30 min needs to be allowed for the Ni ions to be adsorbed onto the PANi composite surface. After that, a further increase in contact time does no difference towards the Ni removal efficiency due to the fixed amount of Ni ions and PANi composite present (Arsalan et al. 2022). The subsequent experiments were conducted at pH 10 and 30 min contact time to examine the effects of other experimental parameters towards the removal efficiency of Ni.

Figure 11 shows the Ni removal efficiency of PANi / TiO₂ / CMC 5 % against different temperatures of 25, 30, 40, and 50 °C. A maximum Ni removal efficiency of 92.59% was achieved at 30 °C, while further increase in temperature had seen a deterioration in the Ni removal efficiency. This is because with an increase in temperature, the polymer structure and active sites of

the PANi composite may be affected which affects the surface chemistry between the Ni ions and the composite active sites (El-Araby et al. 2017). Furthermore, higher temperature may favor desorption of the Ni ions due to the rupture of bonds at high temperature, thus reducing the sorption ability of the PANi composite and lowering its Ni removal efficiency (El-Araby et al. 2017). The remaining experiments were conducted at pH 10, 30 min contact time, and 30 °C to examine the effects of other experimental parameters towards the removal efficiency of Ni.

Lastly, Figure 12 shows the Ni removal efficiency of PANi / TiO₂ / CMC 5 % against different adsorbent weight of 0.005, 0.01, 0.02, 0.03, and 0.05 g. As the adsorbent weight was increased from 0.005 g to 0.01 g, there was an increase in Ni removal efficiency from 88.24 % to 97.88 %, accounting to a maximum adsorption capacity of 21.345 mg/g in this study. This is due to the increase in number of active sites for the uptake of Ni ions (El-Araby et al. 2017). However, upon further addition of adsorbent dosage, the Ni removal efficiency decreased and this could be attributed to the reason that there is a plausible overlapping or aggregation of the adsorbent active sites because of excessive adsorbent particles (El-Araby et al. 2017). As a result, there is a decrease in the composite's ability to adsorb more Ni ions.

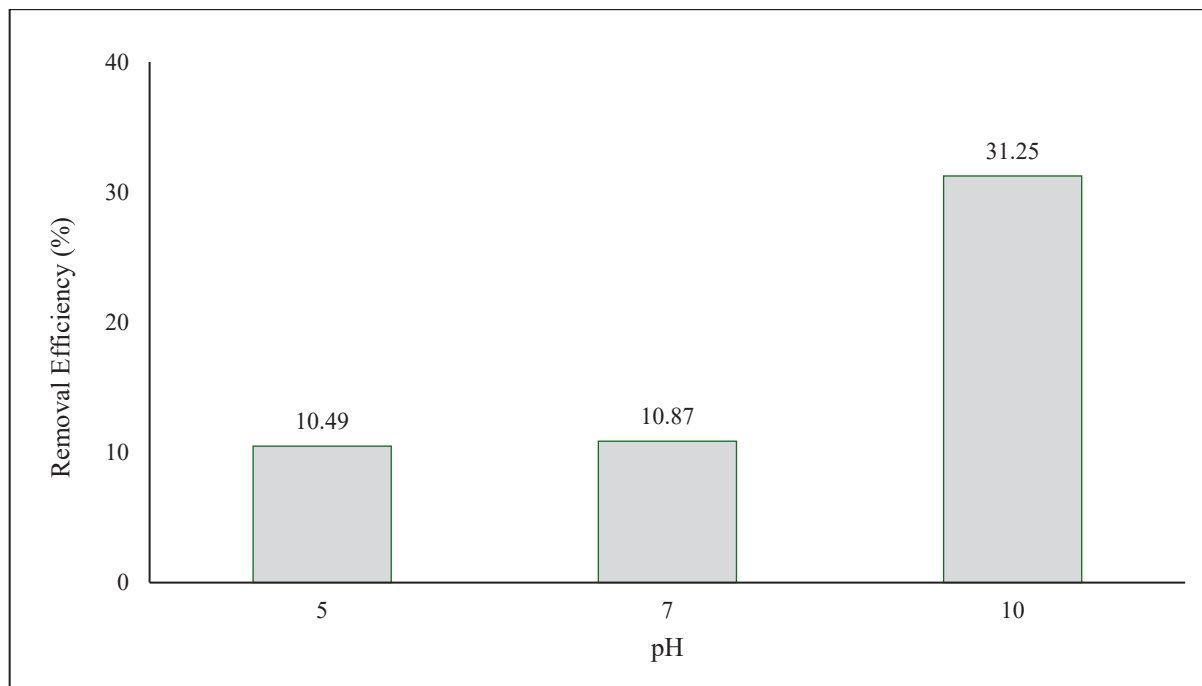
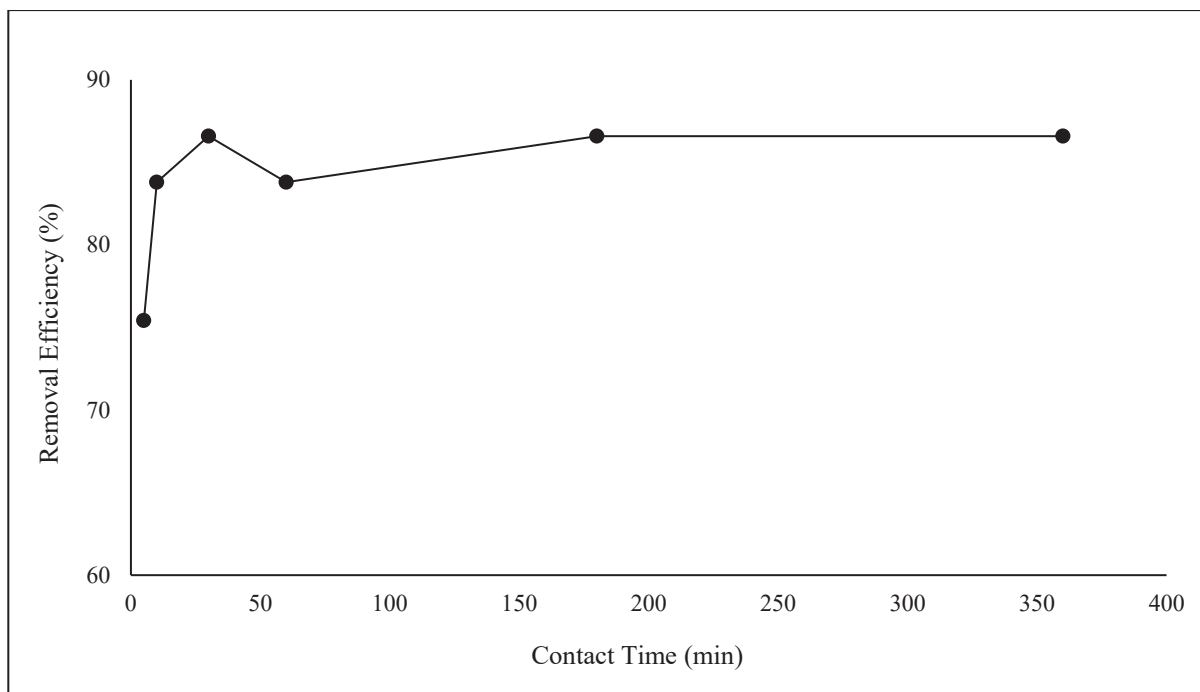
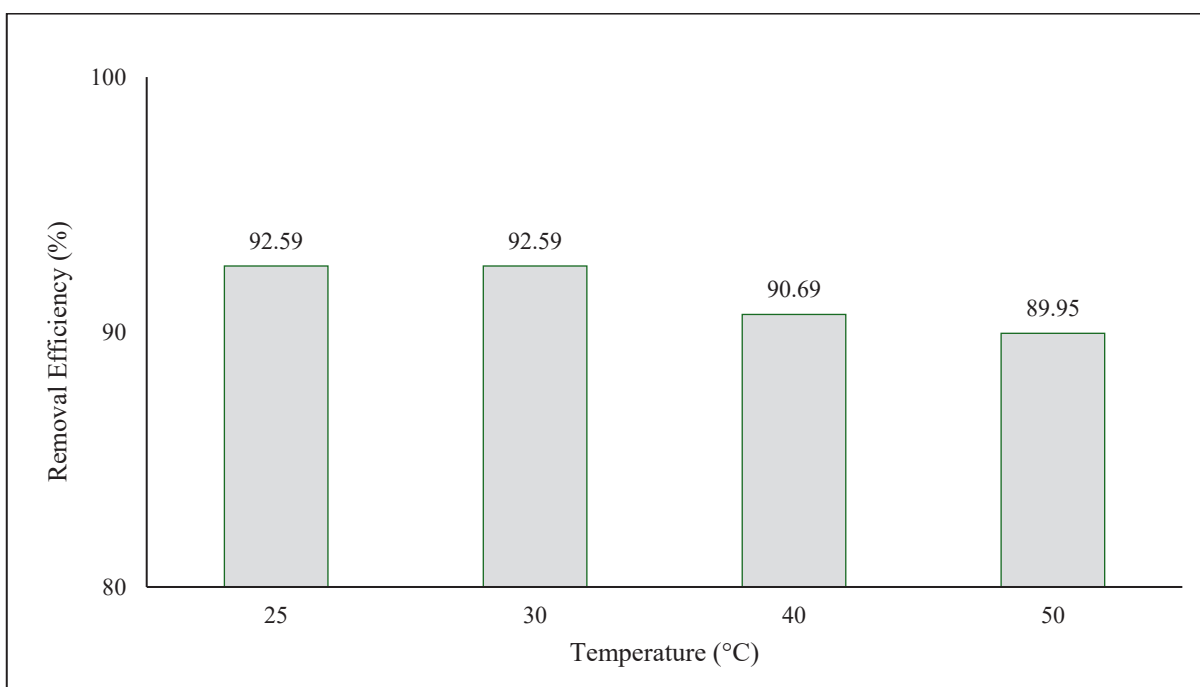


FIGURE 9. Ni removal efficiency of PANi / TiO₂ / CMC 5 % against pH

FIGURE 10. Ni removal efficiency of PANi / TiO₂ / CMC 5 % against contact timeFIGURE 11. Ni removal efficiency of PANi / TiO₂ / CMC 5 % against temperature

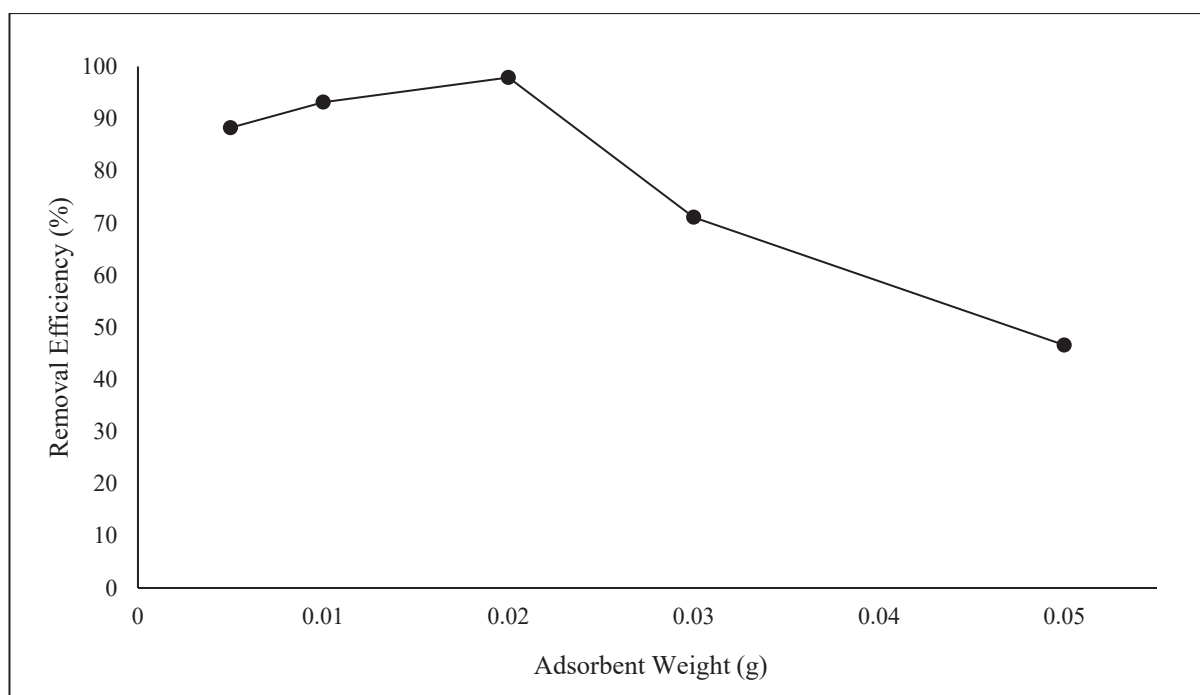


FIGURE 12. Ni removal efficiency of PANi / TiO₂ / CMC 5 % against adsorbent weight

CONCLUSION

As a conclusion, an effective potential heavy metal adsorbent of PANi / TiO₂ / CMC 5 % was successfully synthesized and studied in this research study. All the samples synthesized were successfully investigated by FTIR, UV-Vis, electrical conductivity measurement, XRD, TGA, FESEM, and EDX to determine their chemical structures, oxidation states, electrical conductivity, crystallinity, thermal stability, surface morphology, and incorporation of TiO₂ respectively. Subsequently, the removal efficiencies of Ni and other metal ions by the synthesized samples were successfully measured using FAAS. From the obtained results, it is concluded that PANi / TiO₂ 20 % exhibited the highest Ni removal efficiency of 37.5 % among other samples with different wt % of TiO₂. Then, upon addition of CMC, PANi / TiO₂ / CMC 5 % showed the highest Ni removal efficiency of 89.08%. A maximum Ni removal efficiency of 97.88 % was achieved at pH 10, 30 minutes contact time at a temperature of 30 °C, and with an adsorbent dosage of 0.01 g. This shows that the composite of PANi / TiO₂ / CMC 5 % shows good potential to be applied as adsorbent of the removal of heavy metal ions.

ACKNOWLEDGEMENTS

The author would like to thank Tunku Abdul Rahman University of Management and Technology (TARUMT) for the scholarship and internal grant funding (UC/I/G2023-00125) provided.

REFERENCES

- Abid, N.K. & Hasan, S.M. 2022. Structural properties of prepared PANI/TiO₂ nanocomposite by chemical polymerization. *Iraqi Journal of Physics* 20(3): 29-39.
- Abouelkheir, A.M., Abdelghany, A.M., Ayaad, D.M. & Abdelaal, M.Y.A. 2022. Synthesis and characterization of the thin films containing polyaniline – carboxymethyl cellulose composites. *Egyptian Journal of Chemistry* 65(1): 335-340.
- Ajeel, K.I. & Kareem, Q.S. 2019. Synthesis and characteristics of polyaniline (PANI) filled by graphene (PANI/GR) nanofilms. *IOP Conf. Series: Journal of Physics: Conf. Series* 1234: 012020.
- Andreas, R., Irmanto & Oktaviani, A. 2022. Synthesis, characterization, and activity of the photocatalyst polyaniline (PANI)/TiO₂ in degrading rhodamine B dye. *Science and Technology Indonesia* 7(1): 126-131.

- Anju, V.P. & Narayanankutty, S.K. 2018. Effect of dopant on the properties of polyaniline/carbon nanofiber composites. *Polymer Bulletin* 76(10): 5253-5267.
- Arsalan, M., Siddique, I., Awais, A., Miao, B.J., Khan, I., Badran, M. & Mousa, A.A.A. 2022. Highly efficient PANI-WH novel composite for remediation of Ni(II), Pb(II), and Cu(II) from wastewater. *Frontiers in Environmental Science* 10: 895463.
- Bankole, M.T., Abdulkareem, A.S., Mohammed, I.A., Ochigbo, S.S., Tijani, J.O., Abubakre, O.K. & Roos, W.D. 2019. Selected heavy metals removal from electroplating wastewater by purified and polyhydroxybutyrate functionalized carbon nanotubes adsorbents. *Scientific Reports* 9: 4475.
- Barik, A., Solanki, P.R., Kaushik, A., Ali, A., Pandey, M.K., Kim, C.G. & Malhotra, B.D. 2010. Polyaniline-carboxymethyl cellulose nanocomposite for cholesterol detection. *Journal of Nanoscience and Nanotechnology* 10(10): 6479-6488.
- Budi, S., Fitri, E., Paristiowati, M., Cahyana, U., Pusparini, E., Nasbey, H. & Imaddudin, A. 2017. Surface area and conductivity of polyaniline synthesized under UV irradiation. *IOP Conference Series: Materials Science and Engineering* 172: 012049.
- Chang, F.H., Wang, H.J., Wang, S.L., Wang, Y.C., Hsieh, D.P.H., Chang, L.W. & Ko, Y.C. 2006. Survey of urinary nickel in residents of areas with a high density of electroplating factories. *Chemosphere* 65: 1723-1730.
- Costa, E.M., Pereira, C.F., Ribeiro, A.A., Casanova, F., Freixo, R., Pintado, M. & Ramos, O.L. 2022. Characterization and evaluation of commercial carboxymethyl cellulose potential as an active ingredient for cosmetics. *Applied Sciences* 12(13): 6560.
- Costa, J.M., Costa, J.G.R. & Neto, A.F.A. 2022. Techniques of nickel (II) removal from electroplating industry wastewater: Overview and trends. *Journal of Water Process Engineering* 46: 102593.
- Deesaen, P. 2015. Effects of synthesis time and crystallinity on the Ni (II) sorption performance of sodium titanate ion-exchange compounds. Master Dissertation, Sirindhorn International Institute of Technology Thammasat University (Unpublished).
- Debnath, S., Ballav, N., Maity, A. & Pillay, K. 2015. Development of a polyaniline-lignocellulose composite for optimal adsorption of Congo red. *International Journal of Biological Macromolecules* 75: 199-209.
- El-Araby, H.A., Ibrahim, A.M.M.A., Mangood, A.H. & Abdel-Rahman, A.A.H. 2017. Sesame husks as adsorbent for copper(II) ions removal from aqueous solution. *Journal of Geoscience and Environment Protection* 5: 109-152.
- Helmy, A.K., ElBatal, H.A., Elbatal, F.H., Ouis, M.A., Gamal, A.A. & Abd El-Salam, H.M. 2021. Preparation and characterization of some composite phosphate glass-polyaniline derivatives studying their antimicrobial activity. *Egyptian Journal of Chemistry* 64(9): 5315-5326.
- Jayamurugan, P., Mariappan, R., Deivanayagi, S., Ponnuswamy, V., Maadeswaran, P., Chavali, M. & Subba Rao, Y.V. 2020. Effect of dopant concentration on polyaniline/poly(4-styrene sulfonic acid) composite for ammonia gas detection. *Polymers and Polymer Composites* 28(8-9): 645-653.
- Khan, M.I., Almesfer, M.K., Elkhaleefa, A., Shigidi, I., Shamim, M.Z., Ali, I.H. & Rehan, M. 2021. Conductive polymers and their nanocomposites as adsorbents in environmental applications. *Polymers* 13: 3810.
- Kruszelnicka, I., Ginter-Kramarczyk, D., Gora, W., Staszak, K., Baraniak, M., Lota, G. & Regel-Rosocka, M. 2022. Removal of nickel (II) from industrial wastewater using selected methods: A review. *Chemical and Process Engineering* 43(4): 437-448.
- Li, J.R., Fang, L.J., Tait, W.R., Sun, L.Y., Zhao, L.H. & Qian, L.Y. 2017. Preparation of conductive composite hydrogels from carboxymethyl cellulose and polyaniline with a nontoxic crosslinking agent. *RSC Advances* 7: 54823-54828.
- Li, N., Yuan, M.J., Lu, S., Xiong, X.L., Xie, Z.G., Liu, Y.S. & Guan, W. 2023. Highly effective removal of nickel ions from wastewater by calcium-iron layered double hydroxide. *Frontiers in Chemistry* 10: 1089690.
- Lv, H.M., Wei, Z.Q., Han, C.P., Yang, X.L., Tang, Z.J., Zhang, Y.T., Zhi, C.Y. & Li, H.F. 2023. Cross-linked polyaniline for production of long lifespan aqueous iron organic batteries with electrochromic properties. *Nature Communications* 14: 3117.
- Megha, R., Ravikiran, Y.T., Kotresh, S., Vijaya Kumari, S.C., Raj Prakash, H.G. & Thomas, S. 2017. Carboxymethyl cellulose: An efficient material in enhancing alternating current conductivity of HCl doped polyaniline. *Cellulose* 25: 1147-1158.
- Megha, R., Ravikiran, Y.T., Vijaya Kumari, S.C., Raj Prakash, H.G., Ramana, C.H.V.V. & Thomas, S. 2018. Enhancement in alternating current conductivity of HCl doped polyaniline by modified titania. *Composite Interfaces* 26(4): 309-324.
- Monfared, A.H. & Jamshidi, M. 2019. Synthesis of polyaniline/titanium dioxide nanocomposite (PANI/TiO₂) and its application as photocatalyst in acrylic pseudo paint for benzene removal under UV/VIS lights. *Progress in Organic Coatings* 136: 105257.
- Moosavi, S., Lai, C.W., Gan, S.Y., Zamiri, G., Pivezhani, O.A. & Johan, M.R. 2020. Application of efficient magnetic particles and activated carbon for dye removal from wastewater. *ACS Omega* 5(33): 20684-20697.
- Noman, E., Al-Gheethi, A., Mohamed, R.M.S.R., Al-Sahari, M., Hossain, M.S., Vo, D.V.N. & Naushad, M. 2022. Sustainable approaches for nickel removal from wastewater using bacterial biomass and nanocomposite adsorbents: A review. *Chemosphere* 291(Part 1): 132862.

- Olad, A., Bastanian, M., Aber, S. & Zebhi, H. 2021. Ion-crosslinked carboxymethyl cellulose/polyaniline bio-conducting interpenetrated polymer network: Preparation, characterization and application for an efficient removal of Cr(VI) from aqueous solution. *Iranian Polymer Journal* 30: 105-119.
- Peng, H., Ma, G.F., Ying, W.M., Wang, A.D., Huang, H.H. & Lei, Z.Q. 2012. *In situ* synthesis of polyaniline/sodium carboxymethyl cellulose nanorods for high-performance redox supercapacitors. *Journal of Power Sources* 211: 40-45.
- Qasem, N.A.A., Mohammed, R.H. & Lawal, D.U. 2021. Removal of heavy metal ions from wastewater: A comprehensive and critical review. *Nature Partner Journals Clean Water* 4: 36.
- Rahman, M.L., Wong, Z.J., Sarjadi, M.S., Soloi, S., Arshad, S.E., Bidin, K. & Musta, B. 2021. Heavy metals removal from electroplating wastewater by waste fiber-based poly(amidoxime) ligand. *Water* 13: 1260.
- Rajoria, S., Vashishtha, M. & Sangal, V.K. 2022. Treatment of electroplating industry wastewater: A review on the various techniques. *Environmental Science and Pollution Research* 29: 72196-72246.
- Samadi, A., Xie, M., Li, J.L., Shon, H.Y., Zheng, C.M. & Zhao, S.F. 2021. Polyaniline-based adsorbents for aqueous pollutants removal: A review. *Chemical Engineering Journal* 418: 129425.
- Sambaza, S.S., Maity, A. & Pillay, K. 2020. Polyaniline-coated TiO₂ nanorods for photocatalytic degradation of bisphenol A in water. *ACS Omega* 5(46): 29642-29656.
- Scholes, D.T., Yee, P.Y., Lindemuth, J.R., Kang, H.Y., Onorato, J., Ghosh, R., Luscombe, C.K., Spano, F.C., Tolbert, S.H. & Schwartz, B.J. 2017. The effects of crystallinity on charge transport and the structure of sequentially processed F₄TCNQ-doped conjugated polymer films. *Advanced Functional Materials* 27(44): 1702654.
- Singh, R., Jasrotia, R., Singh, J., Mittal, S. & Singh, H. 2024. Recyclable magnetic nickel ferrite-carboxymethyl cellulose-sodium alginate bio-composite for efficient removal of nickel ion from water. *Journal of Dispersion Science and Technology* doi:10.1080/01932691.2024.2320302
- Su, B.T., Min, S.X., She, S.X., Tong, Y.C. & Bai, J. 2007. Synthesis and characterization of conductive polyaniline/TiO₂ composite nanofibers. *Frontiers Chemistry China* 2(2): 123-126.
- Tale, B.U., Nemade, K.R. & Tekade, P.V. 2021. The comprehensive study of titanium oxide doped conducting polymers nanocomposites for photovoltaic applications. *Polymer-Plastics Technology and Materials* 60(16): 1775-1784.
- Tanzifi, M., Tavakkoli Yaraki, M., Karami, M., Karimi, S., Deghani Kiadehi, A., Karimipour K. & Wang, S. 2018. Modelling of dye adsorption from aqueous solution on polyaniline/carboxymethyl cellulose/TiO₂ nanocomposites. *J. Colloid Interface Sci.* 519: 154-173.
- Wei, W., Yang, L., Zhong, W., Cui, J. & Wei, Z. 2015. Mechanism of enhanced humic acid removal from aqueous solution using poorly crystalline hydroxyapatite nanoparticles. *Digest Journal of Nanomaterials and Biostructures* 10(2): 663-680.
- Yadav, A.K., Mohammad, N. & Khanna, P.K. 2023. Novel synthesis of polyaniline/tellurium (PANI/Te) nanocomposite and its EMI shielding behaviour. *Material Advance* 4: 4409-4416.
- Yuwono, S.D., Wahyuningsih, E., Noviany Kiswandono, A.A., Simanjuntak, W. & Hadi, S. 2020. Characterization of carboxymethyl cellulose (CMC) synthesized from microcellulose of cassava peel. *Materiale Plastice* 57(4): 225-235.
- Zare, E.N., Motahari, A. & Sillanpaa, M. 2018. Nanoadsorbents based on conducting polymer nanocomposites with main focus on polyaniline and its derivatives for removal of heavy metal ions/dyes: A review. *Environmental Research* 162: 173-195.

*Corresponding author; email: phangsw@tarc.edu.my